Paper accepted for presentation at 2009 IEEE Bucharest Power Tech Conference, June 28th - July 2nd, Bucharest, Romania

Robust UPFC Controller Design Using Quantitative Feedback Theory Method

S. A. Taher, Member, IEEE, S. Akbari, Member, IEEE, A. Ketabi, R. Hematti and A. Abdolalipour

***Abstract*—an industrial plant, such a power system, always contains parametric uncertainties. In the design of a controller the uncertainties must be considered. Otherwise, if the real plant differs from the assumed plant model, a controller designed based on classical controller design approaches may not ensure the stability of the overall system. In this paper a robust controller, based on the Quantitative Feedback Theory (QFT) approach is proposed for the design of UPFC controllers (power – flow and DC-voltage regulator). As an example, we have designed a case for the system to compare the proposed method with a conventional method (classical P-I controller). Validity of the proposed method has been confirmed by linear and nonlinear time domain simulation results.**

***Index Term s*-- Unified Power Flow Controller (UPFC); Power System Oscillations; Quantitative Feedback Theory (QFT); Flexible AC Transmission Systems (FACTS).**

I. INTRODUCTION

THE Flexible AC Transmission Systems (FACTS) based on power electronics offer an opportunity to enhance controllability, stability, and power transfer capability of Ac transmission systems [1]. The Unified Power Flow Controller (UPFC), which is the most versatile FACTS device, has the capabilities of controlling power flow in the transmission line, improving the transient stability, mitigating system oscillation and providing voltage support [2-4].

PID is the most commonly used control algorithm in the process industry. Also, this technique is used to control the FACTS devices [5]. However, the nonlinear nature of well as the uncertainties that exist in the system make it difficult to design an effective controller for the FACTS that guarantees fast and stable regulation under all operating conditions. A major source of difficulty is that open-loop plant may change. In particular, inaccuracy in plant may cause problems because the plant is part of the feedback loop. To deal with such a problem, instead of using a single model plant, an uncertain model should be considered. This problem has led to the study of applying adaptive controllers for instance [6, 7], nonlinear controllers for instance [8] in the power system stability control. Also, during past decade, the H_∞ optimal robust control design has received increasing attention in power systems. Most of above methods have been applied in power systems and some of these efforts have contributed to the design of supplementary control for SVC using mixed sensitivity [9], applying μ-synthesis for SVC in order to voltage control design [10] and supplementary control design for SVC and STATCOM [11].

In this paper a robust controller, based on the Quantitative Feedback Theory (QTF) approach is proposed for the design of UPFC controllers (power–flow and DC-voltage regulator). In this method plant uncertainty is considered to QFT bounds and then controller design based these bounds. Because we have considered whole of the plant uncertainty in design of controller, so with change of the plant parameters, we will have a good response in all of system uncertainty area. As an example, a single-machine infinite-bus (SMIB) power system installed with a UPFC is considered for case study and QFT method is used to design a robust controller for UPFC in this system. To show influence of proposed method, the proposed method is compared to conventional method. Based on the result of simulation, the validity of the proposed method has been confirmed.

II. SYSTEM UNDER STUDY

Fig. 1 shows a SMIB power system with UPFC installed [1]. The UPFC is installed in one of the two parallel transmission lines.

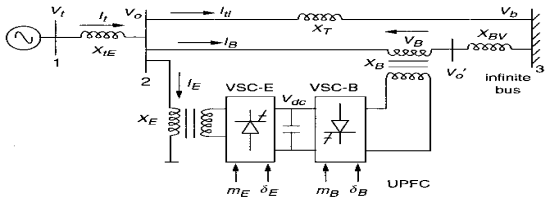

Fig. 1. A single machine infinite bus (SMIB) power system installed with an UPFC in one of the lines

This configuration, comprising two parallel transmission lines, permits the control of real and reactive power flow through a line. The static excitation system, model type IEEE – ST1A, has been considered. The UPFC is assumed to be based on pulse width modulation (PWM) converters. The nominal loading condition and system parameters are given in Appendix I.

This work was supported in part by the Department of Electrical Engineering, University of Kashan.

S. A. Taher, S. Akbari, A. Ketabi, R. Hematti and A. Abdolalipour are with the Department of Electrical Engineering, University of Kashan, Kashan, Iran (e-mail: sataher@kashanu.ac.ir, s-akbari@kashanu.ac.ir).

978-1-4244-2235-7/09/$25.00 ©2009 IEEE

III. DYNAMIC MODEL OF THE SYSTEM WITH UPFC

A. Non-Linear Dynamic Model

A non-linear dynamic model of the system is derived by disregarding the resistances of all components of the system (generator, transformer, transmission lines, and shunt and series converter transformers) and the transients of the transmission lines and transformers of the UPFC. The nonlinear dynamic model of the system using UPFC is given below [12]:

$$\dot{\omega} = \frac{(P_m - P_e - D\Delta\omega)}{M} \tag{1}$$

$$\dot{\delta} = \omega_0(\omega - 1) \tag{2}$$

$$\dot{E}'_q = \frac{(-E_q + E_{fd})}{T'_{do}} \tag{3}$$

$$\dot{E}_{fd} = \frac{-E_{fd} + K_a(V_{ref} - V_t)}{T_a} \tag{4}$$

$$\dot{V}_{dc} = \frac{3m_E}{4C_{dc}}\left(\sin(\delta_E)I_{Ed} + \cos(\delta_E)I_{Eq}\right) + \frac{3m_B}{4C_{dc}}\left(\sin(\delta_B)I_{Bd} + \cos(\delta_B)I_{Bq}\right) \tag{5}$$

The equation for real power balance between the series and shunt converters is given as

$$\mathrm{Re}\left(V_B I_B^* - V_E I_E^*\right) = 0 \tag{6}$$

B. Linear Dynamic Model

A linear dynamic model is obtained by linearising the non-linear model around an operating condition. The linearised model is given below:

$$\Delta\dot{\delta} = w_0 \Delta w \tag{7}$$

$$\Delta\dot{w} = (-\Delta P_e - D\Delta w)/M \tag{8}$$

$$\Delta\dot{E}'_q = (-\Delta E_q + \Delta E_{fd})/T'_{do} \tag{9}$$

$$\Delta\dot{E}_{fd} = -\frac{1}{T_A}\Delta E_{fd} - \frac{K_A}{T_A}\Delta V \tag{10}$$

$$\Delta\dot{v}_{dc} = K_7\Delta\delta + K_8\Delta E'_q - K_9\Delta v_{dc} + K_{ce}\Delta m_E + K_{c\delta e}\Delta\delta_E + K_{cb}\Delta m_B + K_{c\delta b}\Delta\delta_B \tag{11}$$

Where

$$\Delta P_e = K_1\Delta\delta + K_2\Delta E'_q + K_{pd}\Delta v_{dc} + K_{pe}\Delta m_E + K_{p\delta e}\Delta\delta_E + K_{pb}\Delta m_B + K_{p\delta b}\Delta\delta_B$$

$$\Delta E_q = K_4\Delta\delta + K_3\Delta E'_q + K_{qd}\Delta v_{dc} + K_{qe}\Delta m_E + K_{q\delta e}\Delta\delta_E + K_{qb}\Delta m_B + K_{q\delta b}\Delta\delta_B$$

$$\Delta V_t = K_5\Delta\delta + K_6\Delta E'_q + K_{vd}\Delta v_{dc} + K_{ve}\Delta m_E + K_{v\delta e}\Delta\delta_E + K_{vb}\Delta m_B + K_{v\delta b}\Delta\delta_B$$

Fig. 2 shows the transfer function model of the system including UPFC. The model has 28 constants denoted by K. These constants are functions of the system parameters and the initial operating condition. The control vector u is defined as follows:

$$u = [\Delta m_E \quad \Delta\delta_E \quad \Delta m_B \quad \Delta\delta_B]^T \tag{12}$$

Where

Δm_B : Deviation in pulse width modulation index m_B of series inverter. By controlling m_B, the magnitude of series-injected voltage can be controlled.

$\Delta\delta_B$: Deviation in phase angle of injected voltage.

Δm_E : Deviation in pulse width modulation index m_E of shunt inverter. By controlling m_E, the output voltage of the shunt converter is controlled.

$\Delta\delta_E$: Deviation in phase angle of the shunt inverter voltage.

The series and shunt converters are controlled in a coordinated manner to ensure that the real power output of the shunt converter is equal to the power input to the series converter. The fact that the DC-voltage remains constant ensures that this equality is maintained.

It may be noted that K_{pu}, K_{qu}, K_{vu} and K_{cu} in Fig. 2 are the row vectors defined below:

$$K_{pu} = [K_{pe} \quad K_{p\delta e} \quad K_{pb} \quad K_{p\delta b}]$$

$$K_{qu} = [K_{qe} \quad K_{q\delta e} \quad K_{qb} \quad K_{q\delta b}]$$

$$K_{vu} = [K_{ve} \quad K_{v\delta e} \quad K_{vb} \quad K_{v\delta b}]$$

$$K_{cu} = [K_{ce} \quad K_{c\delta e} \quad K_{cb} \quad K_{c\delta b}]$$

And : $u = [\Delta m_E \quad \Delta\delta_E \quad \Delta m_B \quad \Delta\delta_B]^T$.

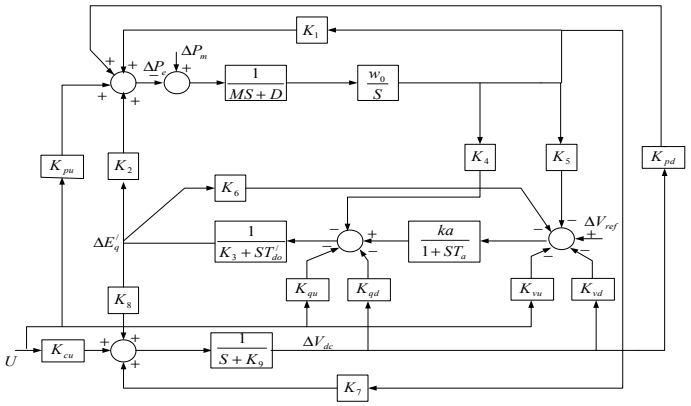

Fig. 2. Transfer function model of the system including UPFC

C. Dynamic Model in State-Space Form

The dynamic model of the system in state-space from transfer-function model is as (13).

$$\begin{bmatrix} \Delta\dot{\delta} \\ \Delta\dot{w} \\ \Delta\dot{E}'_q \\ \Delta\dot{E}_{fd} \\ \Delta\dot{v}_{dc} \end{bmatrix} = \begin{bmatrix} 0 & w_0 & 0 & 0 & 0 \\ -\frac{K_1}{M} & 0 & -\frac{K_2}{M} & 0 & -\frac{K_{pd}}{M} \\ -\frac{K_4}{T'_{do}} & 0 & -\frac{K_3}{T'_{do}} & \frac{1}{T'_{do}} & -\frac{K_{qd}}{T'_{do}} \\ -\frac{K_A K_5}{T_A} & 0 & -\frac{K_A K_6}{T_A} & -\frac{1}{T_A} & -\frac{K_A K_{vd}}{T_A} \\ K_7 & 0 & K_8 & 0 & -K_9 \end{bmatrix} \times \begin{bmatrix} \Delta\delta \\ \Delta w \\ \Delta E'_q \\ \Delta E_{fd} \\ \Delta v_{dc} \end{bmatrix}$$

$$+ \begin{bmatrix} 0 & 0 & 0 & 0 \\ -\frac{K_{pe}}{M} & -\frac{K_{p\delta e}}{M} & -\frac{K_{pb}}{M} & -\frac{K_{p\delta b}}{M} \\ -\frac{K_{qe}}{T'_{do}} & -\frac{K_{q\delta e}}{T'_{do}} & -\frac{K_{qb}}{T'_{do}} & -\frac{K_{q\delta b}}{T'_{do}} \\ -\frac{K_A K_{vc}}{T_A} & -\frac{K_A K_{v\delta e}}{T_A} & -\frac{K_A K_{vb}}{T_A} & -\frac{K_A K_{v\delta b}}{T_A} \\ Kce & K_{c\delta e} & K_{cb} & K_{c\delta b} \end{bmatrix} \times \begin{bmatrix} \Delta m_E \\ \Delta\delta_E \\ \Delta m_B \\ \Delta\delta_B \end{bmatrix} \tag{13}$$

IV. UPFC CONTROLLERS

The UPFC control system comprises three controllers:

1) Power flow controller
2) DC-voltage regulator controller
3) Power system oscillation-damping controller

A. Power Flow and DC-voltage Regulator Controllers

The UPFC is installed in one of the two lines of the SMIB system. Fig. 3 shows the structure of the power flow controller. The power flow controller regulates the power flow on this line. The real power output of the shunt converter must be equal to the real power input of the series converter or vice versa. In order to maintain the power balance between the two converters, a DC-voltage regulator is incorporated. DC-voltage is regulated by modulating the phase angle of the shunt converter voltage. Fig. 4 shows the structure of the DC-voltage regulator.

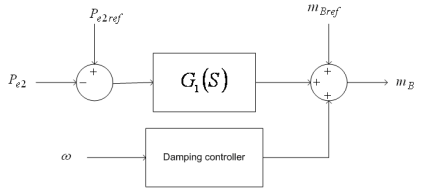

Fig. 3. Power flow controller with damping controller

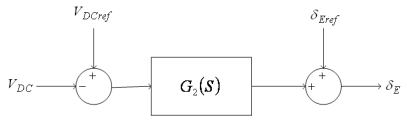

Fig. 4. DC-voltage regulator

B. Power System Oscillation-Damping Controller

A damping controller is provided to improve the damping of power system oscillations. This controller may be considered as a lead-lag compensator [16, 17] or a fuzzy controller block [18]. However an electrical torque in phase with the speed deviation is to be produced in order to improve the damping of the system oscillation. The transfer function block diagram of the damping controller is shown in Fig. 5.

V. ANALYSIS

For nominal operating condition, the eigen-values of the system are obtained (Table 1) usage state-space from transfer-function model of system in (13) and it is clearly seen that the system is unstable.

Table. I. Eigen-values of the closed-loop system without damping controller.

Eigen- values of System without damping controller
-19.2516
0.0308 ± 2.8557i
-0.6695 ± 0.5120i

A. Design of Damping Controller for Stability

The damping controllers are designed to produce an electrical torque in phase with the speed deviation according to phase compensation method. The four control parameters of the UPFC (m_B, m_E, δ_B and δ_B) can be modulated in order to produce the damping torque. In this paper m_B is modulated in order to damping controller design. The speed deviation $\Delta\omega$ is considered as the input to the damping controllers. The structure of damping controller is shown in Fig. 5. It consists of gain, signal washout and phase compensator blocks. The parameters of the damping controller are obtained using the phase compensation technique. The detailed step-by-step procedure for computing the parameters of the damping controllers using phase compensation technique is presented in [16, 17]. Damping controller m_B was designed and obtained as follows (wash-out block is considered). Damping controller of power flow controller with damping ratio of 0.5 is:

$$damping \quad controller = \frac{536.0145 \quad s \quad (s+3.656)}{(s+0.1) \quad (s+4.5)}$$

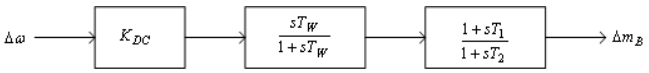

Fig. 5. Structure of damping controller

After employ this damping controller to system, the eigen-values of the system with damping controller are obtained (Table 2) and it is clearly seen that the system is stable.

Table. II. Eigen - values of the closed-loop system with damping controller.

Eigen-values of System with damping controller
-19.3328 , -16.4275 , -2.8609
-0.9251 ± 0.9653i
-0.8814 , -0.1067

VI. DESIGN OF UPFC CONTROLLERS

The UPFC power-flow and DC-voltage regulators are designed independently based on QFT technique. The QFT method is presented in [13-15]. A brief description of the techniques used for the design of UPFC power-flow controller and DC-voltage regulator is presented in next section.

A. Design of Power-Flow Controller

According to QFT method, for the SMIB system, we can consider plant shown in Fig. 6 as an uncertain plant (P_1 is transfer function of system with damping controller). According to previous descriptions and Fig. 6, the structure of control system may be shown as Fig. 7.

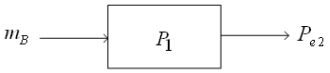

Fig. 6. Open-loop system for power-flow control

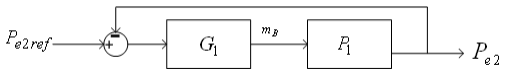

Fig. 7. Closed-loop system for power-flow control

P_1 is the transfer function of the plant which contain parameter uncertainty and obtained usage state space form (13) for any operating point, G_1 is the cascade compensator which to be designed so that the variation of P_{e2} to uncertainty in the plant P_1 is within tolerances, and in this

case, input filter F is not necessary.

first, power system uncertainties must be defined. In order to define the uncertainty, we consider the operating conditions in different active and reactive power and according to these values, defined 6 operating points in this uncertainty area (the area of uncertainty and operating points are given in Appendix I). According to this operating points and plant transfer functions for any operating point (transfer functions of P_1 for operating points), the templates of P_1 for various operating points are obtained by using Matlab software [19] in some frequencies are shown in Fig. 8.

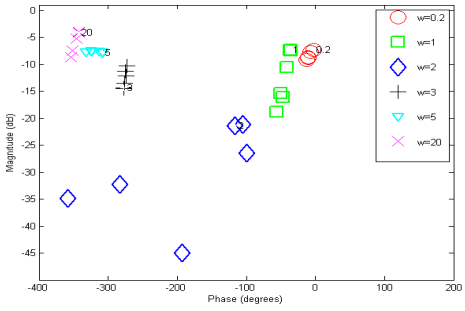

Fig. 8. Templates of plant transfer function P_1

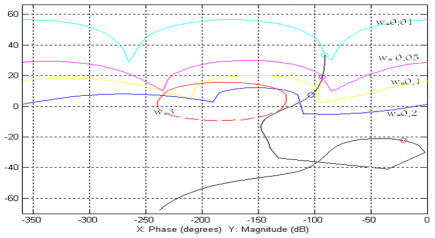

Fig. 9. Bounds and loop shaping for uncertain plant transfer function P_1

1) Trucking Bounds $B_R(j\omega_i)$ and Loop Shaping

According to QFT method, the transfer function of desired upper and lower bounds are as (14) and (15).

$$upper\_bound = \frac{0.81s + 24.3}{30s^2 + 37.8s + 24.3} \tag{14}$$

$$lower\_bound = \frac{15}{s^3 + 60.9s^2 + 54.25s + 15} \tag{15}$$

And the output response (transmission power of line 2) is acceptable if it lies between the upper and lower bounds. With usage templates shown in Fig. 8 and defined upper bound and lower bound for output in (14) and (15), based on desired performance specification, we can obtain tracking bounds according to QFT method. In this plant, because there are no disturbances, therefore it is unnecessary to consider disturbance rejection bounds. In turn the tracking bounds or $B_R(j\omega)$ were considered to composite bounds $B_O(j\omega)$. And also, minimum damping ratios ζ for the dominant roots of the closed-loop system is considered as $\zeta = 1.2$, this amount, on the Nichols chart establishes a region which must not be penetrated by the template of loop shaping (Lo) for all ω. The boundary of this region is referred to as U-contour. U-contour and composite bound $B_O(j\omega)$ and an optimum loop shaping L_{01} according to this bounds and U-contour are shown in Fig. 9. The transfer function for L_{01} is as follow:

$$L_{01} = \frac{384529665455.6973\ (s+13.7)\ (s+19.27)\ (s+3.389)\ (s+0.1)}{s\ (s+19.93)\ (s+1.997)\ (s+14.21)\ (s+.1016)\ (s^2+0.9486s+.5776)} \times \frac{(s^2+0.1423s+4.299)\ (s^2+1.101s+1.188)}{(s^2+2.47s+9.564)\ (s^2+105s+1.182e4)\ (s^2+1e4s+1e8)}$$

And in turn, the compensator G_1 obtained as follow:

$$G_1(s) = \frac{L_{01}(s)}{P_{o1}(s)}$$

$$G_1 = \frac{8.88e11\ (s+3.389)}{s\ (s+1.997)\ (s^2+105s+1.182e4)\ (s^2+1e4s+1e8)}$$

After design of $G_1(S)$, for obtain design objectives, the output response for all operating points must lies between the upper and lower bounds that shown as (14) and (15). The output response for all operating points and desired upper and lower bounds are shown in Fig. 10 for step change in power reference of line 2 ($\Delta P_{e2(ref)}$).

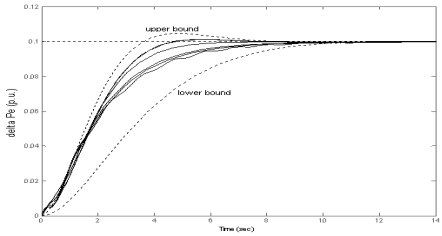

Fig. 10. Response of ΔP for all operating points for $\Delta P_{e2(ref)} = 0.1$

It can be seen clearly in Fig. 10 that design objectives are met and responses in all operating points are between the desired upper and lower bounds.

B. Design of DC-Voltage Regulator Controller

According to previous description and defined uncertainty in system, we can consider plant shown in Fig. 11 as uncertainly plant (P_2 is uncertain transfer function of system with damping controller and without power flow controller).

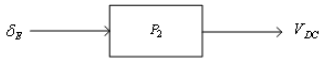

Fig. 11. Open-loop system for DC-voltage regulator

According to previous description and Fig. 11, the structure of control system may be shown as Fig. 12.

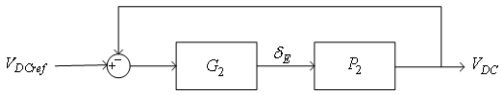

Fig. 12. Closed-loop system for DC-voltage regulator

P_2 is the transfer function of the plant which contain parameter uncertainty and obtained usage state space form (13) for any operating point, G_2 is the cascade compensator which to be designed so that the variation of V_{DC} to uncertainty in the plant P_2 is within tolerances, and in this case, input filter F is not necessary. In previous section the operating points and uncertainty was defined. According to this operating points and plant transfer functions for any

operating point (P_2), the templates of P_2 for various operating points in some frequencies are shown in Fig. 13.

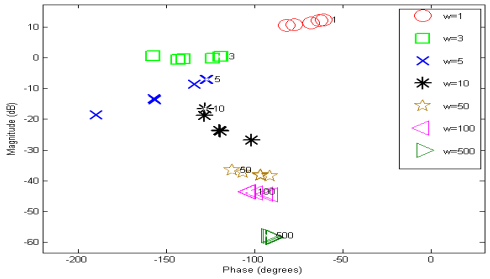

Fig. 13. Templates of plant transfer function P_2

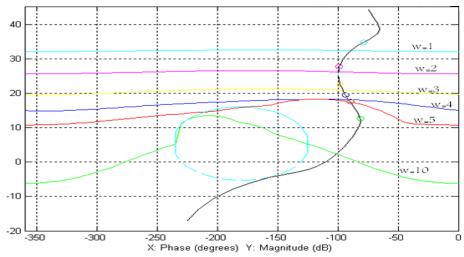

Fig. 14. Bounds and loop shaping for plant transfer function P_2

1) Disturbance Rejections Bounds and Loop Shaping

In this case, because V_{DCref} does not change in real or actual and simulation systems, so, we consider just disturbance rejection bounds for design, and the tracking models are not necessary for this design. Output response (DC-voltage between series and shunt converter) is acceptable if the magnitude of the output to be below the limits given by disturbance rejection models. Based on desired performance specification, we can obtain disturbance rejections bounds according to QFT method. In this plant, because there is not any step to input (V_{DCref}), in turn it is not necessary to consider tracking bounds. In turn the disturbance rejections bounds or $B_D(j\omega_i)$ were considered as composite bounds $B_O(j\omega)$. The U-contour and composite bound $B_O(j\omega)$ and an optimum loop shaping L_{02} according to this bounds, are shown in Fig. 14. The transfer function for L_{02} is as follow:

$$L_{02}=\frac{1144194.8167\ (s+26.87)\ (s+19.04)\ (s+4.744)\ (s+4.086)}{s\ (s+19.78)\ (s+1)\ (s+15.23)\ (s+30.15)\ (s+.1043)}\times$$
$$\frac{(s+2.477)\ (s+2.098)\ (s+1.152)\ (s+0.322)\ (s+0.1045)}{(s^2+1.216s+0.7165)\ (s^2+3.53s+7.036)\ (s^2+119.3s+2.127e4)}$$

And in turn, the compensator G_2 obtained as follow:

$$G_2(s)=\frac{L_{02}(s)}{P_{o2}(s)}$$

$$G_2=\frac{1845534.5\ (s+2.477)\ (s+2.098)\ (s+0.323)}{s\ (s+30.15)\ (s+1)\ (s^2+119.3s+2.127e4)}$$

It should be noted that in section III-B a linear dynamic model is developed and the control vector in (12) contains angle and modulation indexes for both shunt and series inverters. However in section VI only controllers for the shunt inverter angle and series inverter modulation index are designed. Therefore shunt inverter modulation index and series inverter angle are set on the initial values (the initial parameter given in Appendix I) and considered constant in the simulation time.

VII. SIMULATION RESULTS

In this section different comparative cases are examined to show the effectiveness of proposed QFT controllers. These cases have been evaluated extensively by linear and nonlinear time domain simulation, using commercially available software package [19]. Each simulation result presented in this section consists of two different plots (i.e.: conventional UPFC (C-UPFC) and QFT-UPFC), for comparative studies. In conventional method, P-I type controller is considered for power-flow controller and DC-voltage regulator. Figs. 15 and 16 show the transfer function of the P-I type DC-voltage regulator and P-I type power-flow controller, respectively. The parameters of the power-flow controller (k_{pp} and k_{pi}) and DC-voltage regulator (k_{dp} and k_{di}) are optimized using genetic algorithm [20]. Optimum values of the proportional and integral gain setting of the power-flow controller are obtained as $k_{pp}=0.5385$ and $k_{pi}=1.8259$. When the parameter of power-flow controller are set at their optimum values. The parameters of DC-voltage regulator are now optimized and obtained as $k_{dp}=0.398$ and $k_{di}=0.5778$. It should be noted that, the damping controller which designed in section V, for stability, is considered in this section with the same structure. And conventional controllers were designed, by application of cited damping controller.

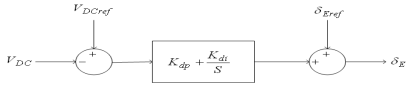

Fig. 15. PI-type DC-voltage regulator

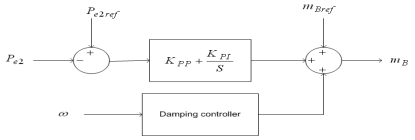

Fig. 16. PI- type power flow controller with damping controller

A. Linear simulation results

In this section time simulations based on small system disturbance (linear simulations) are showed. The Performance of the designed QFT-UPFC and C-UPFC controllers with same damping controller m_B after sudden change in reference power of line 2 and mechanical power, were compared and shown in Figs. 17 to 20.

1) Transient deviation in the power flow on line 2

In this case nominal and heavy loads are considered. Figs. 17 and 18 show the dynamic responses for a 10% step change in reference power on line 2, with QFT-UPFC and C-UPFC, simultaneously.

2) Transient deviation in the mechanical torque (ΔT_m)

Figs. 19 and 20 show the dynamic responses for a 10% step change in reference mechanical torque, with QFT-UPFC and C-UPFC, simultaneously.

Figs. 17 to 20, show that the proposed QFT-UPFC controllers compared to C-UPFC have the best ability to reduce the power system oscillations.

The dynamic results presented in this section were obtained from the linearized model of section III. However a detailed non-linear simulation is required to prove the robustness of the designed controllers. In the next section the nonlinear simulations are presented.

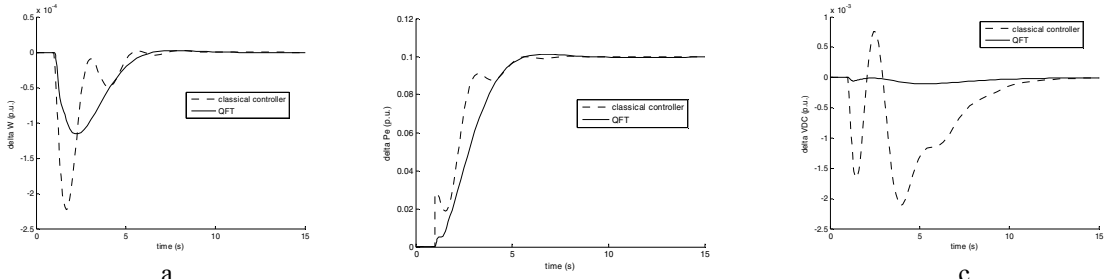

a b c

Fig. 17. Dynamic response for nominal load (operating point 1), following 0.1 step in reference point of the power line 2

a: Dynamic response for $\Delta\omega$ b: Dynamic response for ΔP_{e2} c: Dynamic response for ΔV_{DC}

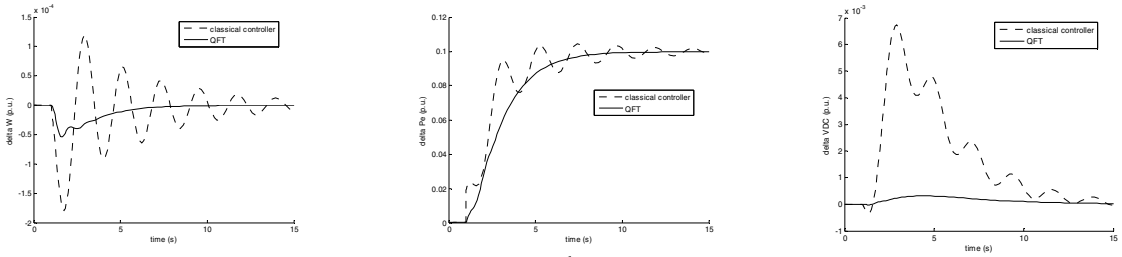

a b c

Fig. 18. Dynamic responses for heavy load (operating point 4), following 0.1 step in reference point of the power line 2

a: Dynamic response for $\Delta\omega$ b: Dynamic response for ΔP_{e2} c: Dynamic response for ΔV_{DC}

a b

Fig. 19. Dynamic responses nominal load (operating point 1), following 0.1 step in mechanical torque

a: Dynamic response for $\Delta\omega$ b: Dynamic response for ΔV_{DC}

a b

Fig. 20. Dynamic responses for heavy load (operating point 4), following 0.1 step in mechanical torque

a: Dynamic response for $\Delta\omega$ b: Dynamic response for ΔV_{DC}

B. Non linear simulation results

The linear model and linear simulations are suitable for study of small disturbance in power system like step change in references of power or so on. But we need nonlinear simulation for study of large disturbance such as short circuit in power system. However in this section the nonlinear simulation results to 3-phase short circuit in

infinite bus and generator terminals are presented.

To study the effectiveness of proposed QFT controllers for large disturbance, the performance of the designed QFT-UPFC and C-UPFC controllers after 3-phase short circuit in infinite bus and generator terminals, were compared and shown in Figs. 21 to 23.

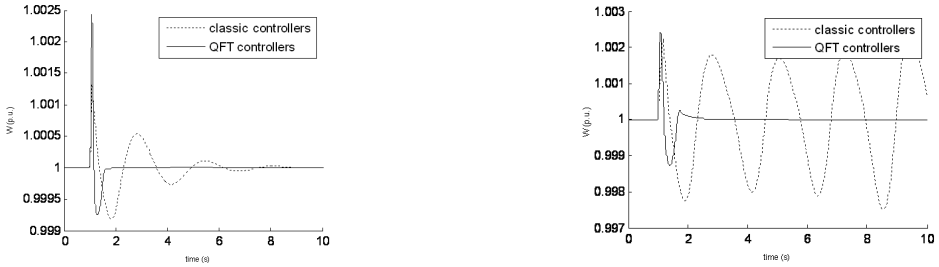

a b

Fig. 21. Dynamic responses for ω with considering transitory 3-phase fault at the infinite bus for nominal load (operating point 1)

a: 5 cycle duration b: 10 cycle duration

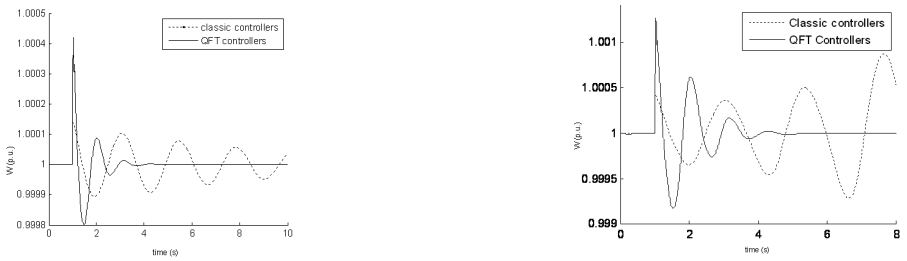

a b

Fig. 22. Dynamic responses for ω with considering transitory 3-phase fault at the infinite bus for heavy load (operating point 4)

a: 5 ms duration b: 15 ms duration

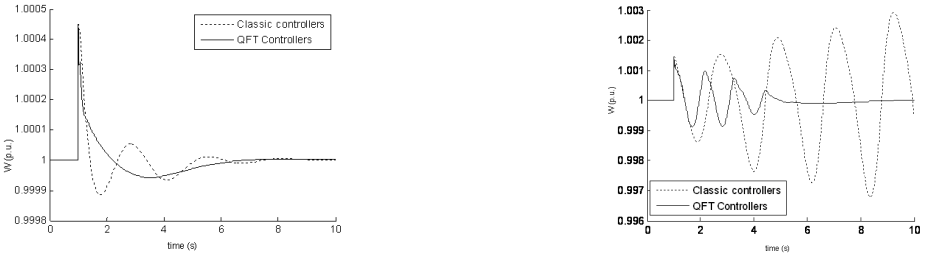

a b

Fig. 23. Dynamic responses for ω with considering transitory 3-phase fault at the generator terminals for nominal load

a: 5 ms duration b: 15 ms duration

Figs. 21 to 23, shows that the proposed QFT-UPFC controllers compared to C-UPFC have the best ability to control power system in the large disturbance time. From the simulation results of this Section system with conventional controllers going unstable for a short circuit. However the QFT controllers are able to stability of system and reduce the power system oscillations.

VIII. CONCLUSION

In this paper, the design of robust controller based on, QFT with application to an UPFC has been carried out for power system. The performance of the controller has been evaluated in comparison with conventional UPFC by time domain simulations. The following issues have been addressed:

1: representation of non-linear characteristics of the system by uncertainty model principle,

2: verification of the QFT controller design by time domain simulations under various operating conditions, and:

3: the results of these studies show that the proposed controller design using QFT method in compare with to conventional method, has an excellent capability in damping of power system oscillations.

APPENDIX I

The nominal parameters and operating conditions of the system are given below:

Generator	$M = 8^{\text{Mj}}/_{\text{MVA}}$	$T'_{do} = 5.044$ s	$X_d = 1$ pu
	$X_q = 0.6$ p.u .	$X'_d = 0.3$ pu	$D = 0$
Excitation system		$K_a = 10$	$T_a = 0.05$s
Transformers		$X_{tE} = 0.1$ pu	$X_E = 0.1$ pu
		$X_B = 0.1$ pu	
Transmission line		$X_{T1} = 1$ pu	$X_{T2} = 1.3$ pu
Operating condition		$P = 0.8$ pu	$Q = 0.15$ pu
		$V_t = 1.032$ pu	
DC link parameter		$V_{Dc} = 2$ pu	$C_{DC} = 3$ pu
UPFC parameters		$m_B = 0.104$	$\delta_B = -55.87^\circ$
		$\delta_E = 26.9^\circ$	$m_E = 1.0233$

The uncertainty area for active and reactive power is as:

$0.7 \le P \le 1.125$ and $0.1 \le Q \le 0.3$

The parameter for operating points:

Operating point 1	$P = 0.8$	$Q = 0.15$	$Vt = 1.032$
Operating point 2	$P = 0.9$	$Q = 0.17$	$Vt = 1.032$
Operating point 3	$P = 1$	$Q = 0.2$	$Vt = 1.032$
Operating point 4	$P = 1.1$	$Q = 0.28$	$Vt = 1.032$
Operating point 5	$P = 1.125$	$Q = 0.285$	$Vt = 1.032$
Operating point 6	$P = 0.7$	$Q = 0.1$	$Vt = 1.032$

(The operating point 1 is nominal operating point)

REFERENCES

[1] N. G. Hingorani and L. Gyugyi, "***Understanding FACTS,"*** IEEE Press, New York, 2000.

[2] L. Gyugyi, *et al*., "***The Unified Power Flow Controller: A New Approach to Power Transmission Control***," *IEEE Transactions on Power Delivery*, vol. 10, no. 2, April 1995, pp. 1085-1093.

[3] L. Gyugyi, "***Unified Power Flow Control Concept for Flexible AC Transmission Systems***," *IEE Proceedings-C*, vol. 139, no. 4, July 1992, pp. 323-331.

[4] A. T. Al-Awami, et al., "A Particle-Swarm-based approach of Power System Stability Enhancement with UPFC", Electrical Power and Energy Systems, vol. 29, 2007, pp. 251-259.

[5] K. L. Liou and Y. Y. Hsu, "***Damping of Generator Oscillation using Static VAR Compensator***," *IEEE Trans. Aero. Electron Sys.,* 1986, vol. 22, no. 5, pp. 605-617.

[6] K. L. Liou and Y. Y. Hsu, "***Damping of Generator Oscillation using an Adaptive Static VAR Compensator***," *IEEE Trans., power Sys*., 1992, 7, (2), pp. 718-725.

[7] J. R. Smith, D. A. Pierre, A. D. Rudberg, I. Sadighi and A. P. Johnson, "***An Enhanced LQ Adaptive VAR Unit Controller for Power System Damping,***" *IEEE Trans., Power Sys*., 1989, 4 (2), pp. 443-451.

[8] Y. Ni, L. Jiao, S. Chen and B. Zhang, "***Application of a Nonlinear PID Controller on STATCOM with a Differential Tracker***," International Conference on Energy Management and Power Delivery, EMPD-98, New York, USA, 1998, pp. 29-34.

[9] Q. Zhao and J. Jiang, "***Robust SVC Controller Design for Improving Power System Damping***," *IEEE Trans., Power Sys*., 1995, 10, (4), pp. 1927-1932.

[10] M. Parniani and M. R. Iravani, "***Optimal Robust Control Design of Static VAR Compensators***," *IEE Proc., Gen. Trans. Dist*. 1998, 145, (3), pp. 301-307.

[11] M. M. Farsangi, Y. H. Song and Y. Z. Sun, "***Supplementary Control Design of SVC and STATCOM using*** H_∞ ***Optimal Robust Control***," International Conference Electric Utility Deregulation and Restructuring and Power Technologies, DRPT 2000, City University London, UK, 2000, pp. 355-360.

[12] N. Tambey and M. L. Kothari, "***Damping of Power System Oscillation with Unified Power Flow Controller (UPFC)***," *IEE Proc. Gene. Trans. Dist*., vol. 150, no. 2, March 2003, pp. 129-140.

[13] J. J. Dazzo and C. H. Houpis, "***Linear Control System Analysis and Design Conventional and Modern***," McGraw Hill, 1988.

[14] I. Horowitz, "***Quantitative Feedback Theory***," *IEEE Proc*., vol. 129, pt. D, no. 6, NOVEMBER 1982.

[15] B. Azvine and R. J. Wynne, "***A Review of Quantitative Feedback Theory as a Robust Control System Design Technique***," Trans. Inst. MC, vol. 14, no. 5, 1992, pp. 265-279.

[16] H. F. Wang, "***Damping Function of Unified Power Flow Controller***," *IEE Proc. Gen. Trans. Dist.*, vol. 146, no. 1, January 1999, pp. 129-140.

[17] Y. N. Yu, "***Electric Power System Dynamics***," Academic Press*, Inc.,* London, 1983.

[18] A. A. Eldamaty, S. O. Faried and S. Aboreshaid, "***Damping Power System Oscillation Using a Fuzzy Logic Based Unified Power Flow Controller***," *IEEE CCECE/CCGEI* 2005, vol. 1, May 2005, pp. 1950-1953.

[19] ***Matlab Software***, The Mathworks, Inc. 2006.

[20] L. H. Randy and E. H. Sue, "***Practical Genetic Algorithms"****,* John Wiley & Sons, Second Edition, 2004.